

Array analysis of epilepsy-associated gangliogliomas reveals expression patterns related to aberrant development of neuronal precursors

Jana Fassunke,¹ Michael Majores,^{1,2} Achim Tresch,³ Pitt Niehusmann,^{1,4} Alexander Grote,⁵ Susanne Schoch¹ and Albert J. Becker¹

¹Department of Neuropathology, ²Department of Pathology, University of Bonn Medical Center, Bonn, ³Gene Center, Ludwig-Maximilians-University, Munich, ⁴Department of Epileptology and ⁵Department of Neurosurgery, University of Bonn Medical Center, Bonn, Germany

Correspondence to: Albert J. Becker, MD, Department of Neuropathology, University of Bonn Medical Center, Sigmund-Freud-Strasse 25, D-53105 Bonn, Germany
E-mail: albert_becker@uni-bonn.de

Gangliogliomas, the most frequent neoplasms in patients with pharmaco-resistant focal epilepsies, are characterized by histological combinations of glial and dysplastic neuronal elements, a highly differentiated phenotype and rare gene mutations. Their molecular basis and relationship to other low-grade brain tumours are not completely understood. Systematic investigations of altered gene expression in gangliogliomas have been hampered by their cellular complexity, the lack of suitable control tissue and of sensitive expression profiling approaches. Here, we have used discrete microdissected ganglioglioma and adjacent control brain tissue obtained from the neurosurgical access to the tumour of identical patients ($n = 6$) carefully matched for equivalent glial and neuronal elements in an amount sufficient for oligonucleotide microarray hybridization without repetitive amplification. Multivariate statistical analysis identified a rich profile of genes with altered expression in gangliogliomas. Many differentially expressed transcripts related to intra- and intercellular signalling including protein kinase C and its target NELL2 in identical ganglioglioma cell components as determined by real-time quantitative RT-PCR (qRT-PCR) and *in situ* hybridization. We observed the LIM-domain-binding 2 (LDB2) transcript, critical for brain development during embryogenesis, as one of the strongest reduced mRNAs in gangliogliomas. Subsequent qRT-PCR in dysembryoplastic neuroepithelial tumours ($n = 7$) revealed partial expression similarities as well as marked differences from gangliogliomas. The demonstrated gene expression profile differentiates gangliogliomas from other low-grade primary brain tumours. shRNA-mediated silencing of LDB2 resulted in substantially aberrant dendritic arborization in cultured developing primary hippocampal neurons. The present data characterize novel molecular mechanisms operating in gangliogliomas that contribute to the development of dysplastic neurons and an aberrant neuronal network.

Keywords: glioneuronal; development; migration; network; epilepsy; dysplastic

Abbreviations: ARF3 = ADP-ribosylation factor 3; DNETs = dysembryoplastic neuroepithelial tumours; GFP = green fluorescent protein; HSJ2 = heat shock 40 kDa protein 4; LDB2 = LIM-domain-binding 2; LMO4 = LIM domain only 4; MMP2 = matrix metalloproteinase 2; NGFR = nerve growth factor receptor; PRKCBI = protein kinase C β -I; ST6GalNAc4 = α -N-acetyl-neuraminyl-2,3- β -galactosyl-1,3-N-acetyl-galactosaminide α -2,6-sialyltransferase; TRIB1 = tribbles homolog 1

Received February 7, 2008. Revised August 19, 2008. Accepted August 20, 2008. Advance Access publication September 26, 2008

Introduction

Gangliogliomas, the most frequent tumours encountered in pharmaco-resistant patients with focal epilepsies are composed of dysplastic neuronal and proliferative, neoplastic glial cells that comprise a considerable spectrum of cellular

and histological architectures (Fig. 1) (Luyken *et al.*, 2003; Becker *et al.*, 2007). Their focal nature and differentiated glioneuronal phenotype, the expression of the stem cell epitope CD34 and the benign clinical course suggest an origin from developmentally compromised or dysplastic

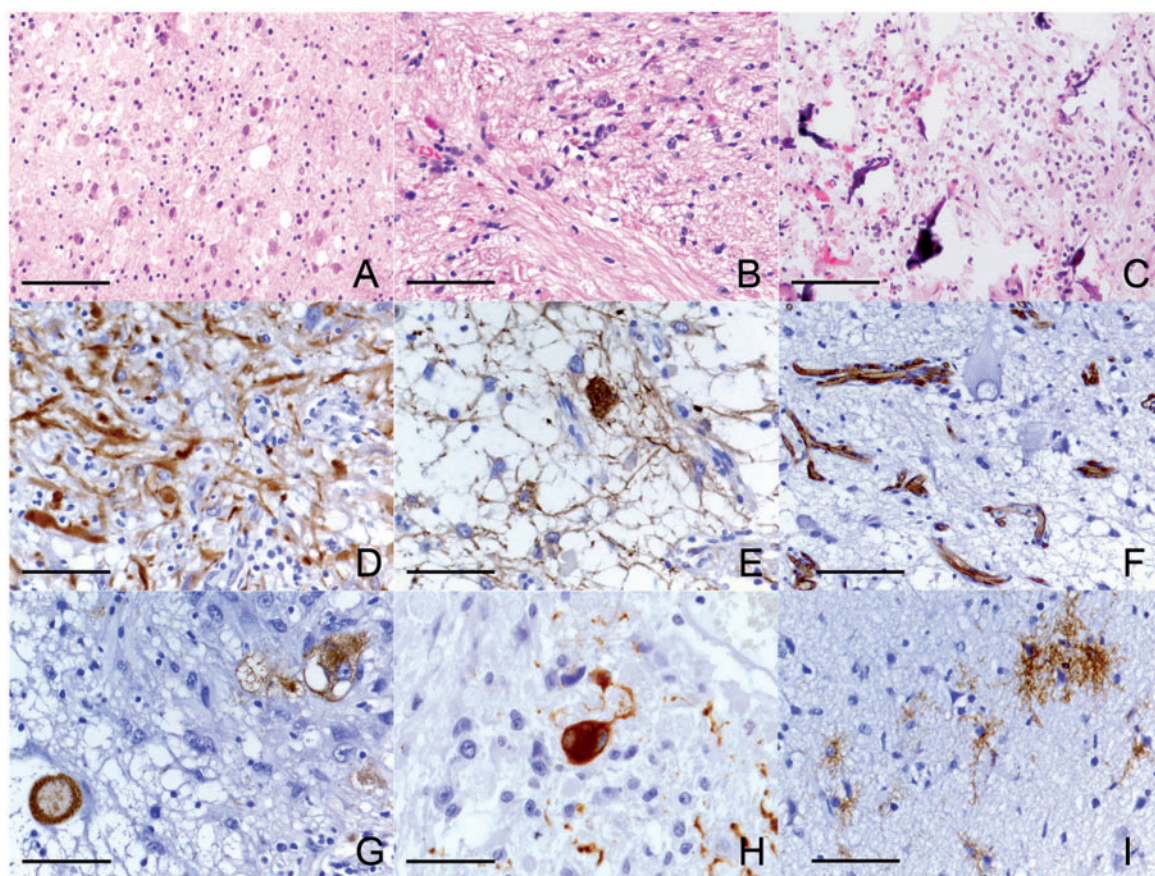


Fig. 1 Histopathological and immunohistochemical characteristics of gangliogliomas. **(A)** Gangliogliomas are characterized by a combination of glial and dysmorphic neuronal elements (haematoxylin–eosin). **(B, C)** These tumours may also show a broad spectrum of histomorphological variants including piloid growth pattern, calcifications as well as neurocytic cells (Becker *et al.*, 2007), features observed in the gangliogliomas included in the present array analysis. **(D–I)** The immunohistochemical profile shows abundant expression of glial fibrillary acid protein by neoplastic glial cells **(D)**; whereas, MAP2 immunolabelling **E** marks only the dysmorphic neurons but not the fibrillary glial cells. Note binucleated dysplastic neurons with perisomatic synaptophysin immunoreactivity **G** and accumulation of neurofilament protein **H**. Whereas, dysmorphic neurons in gangliogliomas often lack expression of CD34 **(F)**, notice CD34-positive blood vessel endothelia, frequent CD34-positive, 'satellite' cells in the vicinity of gangliogliomas suggest a maldevelopmental origin of gangliogliomas **I**. Magnification and scale bars: **A–C**: $\times 200$, 100 μm ; **D–I**: $\times 400$, 50 μm .

precursor lesions (Blümcke *et al.*, 2002; Fassunke *et al.*, 2004). However, so far the molecular basis of gangliogliomas as well as their neuropathological relationship to other primary low-grade brain tumours such as dysembryoplastic neuroepithelial tumours (DNETs) or diffuse and pilocytic astrocytomas (Rorive *et al.*, 2006; Dumas-Duport *et al.*, 2007; Sharma *et al.*, 2007) are poorly understood. Genetic studies have argued against the contribution of mutational events in genes involved in other brain tumours to play a major role in gangliogliomas (Becker *et al.*, 2006). To control seizures, many patients with pharmacoresistant epilepsy due to gangliogliomas have to undergo neurosurgery. The resulting biopsy specimens provide a unique opportunity to analyse the molecular profiles of these glioneuronal tumours.

Expression microarrays enable the comprehensive analysis of transcript alterations (Becker *et al.*, 2003; Lukasiuk *et al.*, 2003; Crino and Becker, 2006; Kang *et al.*, 2007; Aronica *et al.*, 2008). However, central nervous and glioneuronal tumour

tissue samples pose a particular challenge to expression array studies in several regards. The complex cellular composition of glioneuronal tumours needs its equivalent in the control tissue used. In a recent microarray study on gangliogliomas, tissue samples from brain autopsies have been used as control (Aronica *et al.*, 2008), which require careful monitoring for potential variability due to mRNA-degradation and expression differences based on heterogeneity of genetic background of individuals. In an intriguing attempt to overcome cellular heterogeneity on the resulting data, individual ganglioglioma cell components were used for expression array analysis (Samadani *et al.*, 2007). However, this approach relies on the substantial amplification of mRNA and might thereby limit the number of transcripts to be analysed.

In the present analysis, we have included only gangliogliomas, for which pre-existing brain tissue from the neurosurgical access to the neoplasm was available from the same patient. Thereby, we aimed to minimize inter-individual

gene expression variability, which can profoundly contaminate differential gene expression patterns (Cheung *et al.*, 2005; Spielman *et al.*, 2007). Careful microdissection of ganglioglioma and control tissue resulted in mRNA amounts sufficient for high-density oligonucleotide array hybridization (Affymetrix, Santa Barbara, CA, USA) without repetitive mRNA amplification steps. In concert with real-time quantitative RT-PCR (qRT-PCR) and *in situ* hybridization for confirmation and further cellular resolution, we found 94 genes to be differentially expressed in gangliogliomas, including several novel genes of particular interest for the development of these tumours, i.e. protein kinase C and its target NELL2 as well as LIM-domain-binding 2 (LDB2), a transcriptional coactivator critical during embryonal brain development (Ostendorff *et al.*, 2006). The present findings identify novel aberrant gene expression patterns in gangliogliomas that contribute to further elucidate the molecular basis of these tumours and differentiate them from other low-grade brain neoplasms.

Methods

Surgical specimens

Biopsy samples were obtained from ganglioglioma patients with chronic pharmacoresistant temporal lobe epilepsy (TLE) in the Epilepsy Surgery Program at Bonn University (Supplementary Table S1, $n=6$). Surgical removal of tumours was necessary to achieve seizure control in all patients after standardized pre-surgical evaluation using a combination of non-invasive and invasive procedures (Kral *et al.*, 2002; Kral *et al.*, 2003). As for ganglioglioma patients and also for patients with DNETs ($n=7$), informed and written consent was obtained from all patients for additional studies. Procedures were carried out in accordance with the Declaration of Helsinki and were approved by the local ethics committee. Patients have been carefully matched with respect to clinico-epidemiological criteria to minimize structural variability. Each specimen has been subjected to standardized neuropathological evaluation by two independent neuropathologists and classified according to the World Health Organization classification of tumours (Becker *et al.*, 2007; Dumas-Duport *et al.*, 2007).

Oligonucleotide microarray experiments

Transcriptome-wide expression analyses were performed by cRNA oligonucleotide microarrays (Affymetrix) similarly as described in detail before (Becker *et al.*, 2003). Briefly, sample preparation, hybridization to HG U133A microarrays (Affymetrix), washing, staining and scanning in a GeneArray scanner (Agilent, Palo Alto, CA, USA) were performed according to the manufacturer's recommendations. Fresh frozen tissue samples were cut into 12 μm sections and were screened for control and tumour areas after haematoxylin–eosin staining. In order to establish the statistical possibility of pairwise-testing approaches only snap frozen tissue with valuable discrimination between tumour and control tissue from the neurosurgical access of the same patient was involved in this study. RNA was isolated from thin tissue slices using Qiagen RNA Mini Kit (Qiagen, Hilden, Germany) according to the manufacturer's instructions. The RNA quality was evaluated according to several recently established quality

markers, including the 3':5' signal ratios of reference gene transcripts (HUM-GAPDH 3.0, HUM-18S-rRNS 2.6) and RNA integrity number (RIN) (Stan *et al.*, 2006). Due to absence of significant mRNA degradation based on these quality markers including $\text{RIN} \geq 7$ ($\text{RIN}: 7.46 \pm 0.2$), the present samples were suitable for subsequent experiments. Approximately 2.3 μg of each total RNA was subjected to further microarray analysis. After reverse-transcription into cDNA using T7 RNA polymerase promoter sequences, cRNA amplification with biotinylated nucleotides was catalysed by T7 RNA polymerase and cRNA was fragmented to a mean size of 50 bp prior to hybridization to the chips.

Signal intensities for further analysis were determined by the GeneChip Microarray Suite (MAS) 5.0 software (Affymetrix) including RMA analysis. Subsequent data analyses were performed in R (v.1.9.1). Visual inspection of pairwise scatterplots and Q–Q plots confirmed that there were no hybridization failures or outliers, and no substantial rescaling of the data was necessary for array comparability. Cyclic lowess (locally weighted linear regression) was used as a normalization procedure (Yang *et al.*, 2002). After normalization, the expression values showed the typical heavily right-skewed distribution on the absolute scale (Dudoit *et al.*, 2002; Ballman *et al.*, 2004). We excluded low-abundant gene transcripts, i.e. expression values, which had a mean expression value below 100 in both conditions. Apparently, there is no consensus concerning an optimal threshold for expression array analysis. The present conditions are similar to a recent approach (Becker *et al.*, 2003). They represent a reasonable compromise between identification of differentially expressed low-abundant genes and avoiding augmented false positive results (Tang *et al.*, 2002; Miller *et al.*, 2008). This pre-filtering reduces the number of false positives in the low-transcript abundance region, which is prone to a large measurement error. According to an error model of Rocke and Durbin (2001), the error of the log-transformed data was approximately normally distributed for higher transcript abundance. Differential expression was estimated by paired *t*-tests for each transcript using log-transformed expression data. Detailed information on *P*-values for individual genes is presented in Table 1. Accounting for multiple testing issues, the *P*-values were adjusted by the Benjamini–Hochberg algorithm.

Real-time polymerase chain reaction

Relative quantification ($\Delta\Delta C_t$) was carried out for mRNA analysis in gangliogliomas as well as DNETs. In each case, adjacent control tissue of the same patient was obtained. The reference gene β -actin was used for normalization (Fink *et al.*, 1998; Chen *et al.*, 2001). qRT-PCR (ABI PRISM 7700) was carried out in a 13 μl reaction volume containing 6.25 μl SYBR Green PCR Master Mix (Applied Biosystems, Darmstadt, Germany), 0.375 μl forward and reverse primers (10 pmol/ μl ; Supplementary Table S2), 3.0 μl DEPC–H₂O and 2.5 μl cDNA dissolved in DEPC–H₂O. Duplicate reactions were carried out for each transcript. After pre-incubation for 10 min at 95°C, the PCR reaction was performed (20 s at 94°C followed by 30 s at 59°C and 40 s at 72°C, 50 \times). The SYBR Green fluorescence signal was measured in each cycle.

RNA *in situ* hybridization

Cellular resolution of expression patterns was obtained by RNA *in situ* hybridization. Thin tissue slices (12 μm) were cut on a cryostat, thaw-mounted on silane-coated slides, fixed with 4% (w/v) paraformaldehyde in phosphate buffer saline (PBS), dehydrated, and

Table 1 Differentially expressed genes between ganglioglioma and control tissue

Gene Symbol	GenBank ID	Description	Fold change	P-value
Regulation of chromatin state and transcription factors				
FLJ20273	NM.019027.1	RNA-binding protein	2.41	0.0019
TCF3	BE962186	Transcription factor 3	2.05	0.0002
MEIS1	NM.002398.1	Meis homeobox 1	1.76	0.0018
MIDI	AF041209.1	Midline 1 fetal kidney isoform 2	1.74	0.0016
SERTAD2	BGI07456	SERTA domain containing 2	1.67	0.0036
HMGB1	BE311760	High-mobility group box 1	1.56	0.0005
HIVBP2	AL023584	Human immunodeficiency 1 enhancer binding protein 2	0.62	0.0005
HLF	M95585.1	Hepatic leukemia factor	0.51	0.0033
CDY1	AF080597.1	Chromodomain protein, Y-linked, 1	0.42	0.0026
BCL11A	AF080216.1	B-cell CLL/lymphoma 11A	0.37	0.0012
SCAND2	AK022844.1	SCAN domain containing 2	0.32	0.0002
Intracellular signal transduction				
UBE1L	NM.003335.1	Ubiquitin-activating enzyme E1-like	3.65	0.0032
DPYD	NM.000110.2	Dihydropyrimidine dehydrogenase	3.06	0.0010
MS4A6A	NM.022349.1	Membrane-spanning 4-domains, memb. 6A	2.39	0.0035
LOC728866	AL136636.1	Implantation-associated protein	2.10	0.0046
ZAP3	AI703162	YLP motif containing 1	2.04	0.0031
ITPKB	NM.002221.1	Inositol 1,4,5-trisphosphate 3-kinase B	1.83	0.0023
PTPNI3	NM.006264.1	Protein tyrosine phosphatase, non-receptor type 13	1.78	0.0012
GNGI2	BG111761	Guanine nucleotide-binding protein, γ 12	1.69	0.0006
TRAM1	BC000687.1	Translocation-associated membrane protein	1.66	0.0037
SLC25A16	BC001407.1	Solute carrier family 25, member 16	1.57	0.0020
ATP6V0E1	NM.003945.1	ATPase	1.53	0.0045
GLUL	U08626	Glutamate-ammonia ligase (glutamine synthetase)	1.53	0.0046
SYT5	AI659957	Synaptotagmin V	0.66	0.0046
CASQ1	NM.001231.1	Calsequestrin 1 (fast-twitch, skeletal muscle)	0.66	0.0029
ARF3	NM.001659.1	ADP-ribosylation factor 3	0.65	0.0032
NXPH4	AI933199	Neurexophilin 4	0.64	0.0039
SLC25A28	NM.031212.1	Solute carrier family 25, member 28	0.63	0.0046
PRKCI	AI689429	Protein kinase C, iota	0.63	0.0041
AKT3	U79271.1	v-akt murine thymoma viral oncogene homolog 3	0.62	0.0045
TCPI	BF224073	t-complex 1	0.60	0.0005
RASAL1	NM.004658.1	RAS protein activator like 1 (GAP1 like)	0.59	0.0019
HSJ2	AF080569.1	DnaJ (Hsp40) homolog, subfamily B, member 6	0.58	0.0035
ST6GALNAC4	AB035172.1	ST6-N-acetylgalactosaminide α -2,6-sialyltransferase 4	0.58	0.0019
PGAM1	NM.002629.1	Phosphoglycerate mutase 1 (brain)	0.58	0.0002
MCF2	X13230.1	MCF2 cell line-derived transforming sequence	0.54	0.0002
SCAMP5	BE222801	Secretory carrier membrane protein 5	0.51	0.0041
EFHD2	NM.024329.1	EF-hand domain family, member D2	0.51	0.0005
AACS	NM.023928.1	Acetoacetyl-CoA synthetase	0.51	0.0030
STYK1	AF251059.1	Serine/threonine/tyrosine kinase 1	0.50	0.0002
ADCY2	AUI49572	Adenylate cyclase 2 (brain)	0.44	0.0031
MTMR8	NM.004686.1	Myotubularin-related protein 8	0.41	0.0010
HSPA12A	AB007877.1	Heat shock 70 kDa protein 12A	0.41	0.0023
ATP2B2	R52647	ATPase, Ca ⁺⁺ transporting, plasma membrane 2	0.39	0.0021
PRKCBI	MI3975.1	Protein kinase C, β 1	0.34	0.0042
RICH2	NM.014859.1	Rho-type GTPase-activating protein RICH2	0.29	0.0040
HSPH1	BG403660	Heat shock 105 kDa/110 kDa protein 1	0.26	0.0041
Transduction of extracellular signals and cell adhesion				
MMP2	NM.004530.1	Matrix metalloproteinase 2	2.92	0.0002
PLAT	NM.000930.1	Plasminogen activator, tissue	1.78	0.0043
SNAP23	BC003686.1	Synaptosomal-associated protein, 23 kDa	1.78	0.0014
LEPR	U50748.1	Leptin receptor	1.75	0.0031
STAB1	NM.015136.1	Stabilin 1	1.75	0.0042
P2RY5	NM.005767.1	Purinergic receptor P2Y, G-protein coup., 5	1.74	0.0043
MPZL1	BF978611	Myelin protein zero-like 1	1.63	0.0008
FLRT3	NM.013281.1	Fibronectin leucine rich transmem. protein 3	0.61	0.0034
VAMP2	NM.014232.1	Synaptobrevin 2	0.55	0.0040
CYFIP2	AL161999.1	Cytoplasmic FMRI interacting protein 2	0.53	0.0029
SSTR2	BC000256.1	Somatostatin receptor 2	0.50	0.0006

(continued)

Table 1 Continued

Gene Symbol	GenBank ID	Description	Fold change	P-value
CDH8	AB035305.1	Cadherin 8, type 2	0.45	0.0000
GABARAPLI	AFI80519.1	GABA(A) receptor-associated protein like I	0.45	0.0046
NELL2	NM.006159.1	NEL-like 2	0.32	0.0046
SLCIA6	NM.005071.1	Solute carrier family 1, member 6	0.30	0.0031
Control of cell cycle and proliferation				
TP53I3	BC000474.1	Tumour protein p53 inducible protein 3	3.74	0.0035
ALK	NM.004304.2	Anaplastic lymphoma kinase (Ki-I)	2.55	0.0038
INHBB	NM.002193.1	Inhibin, β B	2.21	0.0024
TRIB1	NM.025195.1	Tribbles homolog 1 (Drosophila)	1.89	0.0025
EDNRA	NM.001957.1	Endothelin receptor type A	1.76	0.0001
CKLF	NM.016951.2	Chemokine-like factor	1.73	0.0042
PARP4	NM.006437.2	Poly (ADP-ribose) polymerase family, member 4	1.69	0.0001
NEK9	AI117502.1	NIMA (never in mitosis gene a)-related kinase 9	1.59	0.0020
IGFIR	NM.000875.2	Insulin-like growth factor I receptor	1.54	0.0036
RMNDI	NM.017909.1	Meiotic nuclear division I homolog	0.64	0.0011
NOV	NM.002514.1	Nephroblastoma overexpressed gene	0.45	0.0012
ACTR3B	NM.020445.1	ARP3 actin-related protein 3 homolog B (yeast)	0.44	0.0047
Development and differentiation				
NGFR	NM.002507.1	Nerve growth factor receptor	10.34	0.0011
COL1A2	AA788711	Collagen, type I, α 2	2.17	0.0043
CDI4	NM.000591.1	CDI4 molecule	2.14	0.0005
EPB41L2	NM.001431.1	Erythrocyte membrane protein band 4.1-like 2	1.52	0.0027
FAM128B	BG255188	Family with sequence similarity 128, member B	0.62	0.0011
MAPT	NM.016835.1	Microtubule-associated protein tau	0.62	0.0006
CLPTM1	BC004865.1	Cleft lip and palate-associated transmembrane protein 1	0.60	0.0016
LMO4	BC003600.1	LIM domain only 4	0.51	0.0041
LDB2	NM.001290.1	LIM domain binding 2	0.32	0.0045
NEUROD6	NM.022728.1	Neurogenic differentiation 6	0.24	0.0004
Varia				
CDI63	NM.004244.1	CDI63 molecule	2.47	0.0037
TNIP2	AA522816	TNFAIP3 interacting protein 2	1.66	0.0020
CLEC7A	AF313468.1	C-type lectin domain family 7, member A	1.61	0.0033
URBI	NM.014825.1	URBI ribosome biogenesis I homolog	0.66	0.0042
TMEM70	NM.017866.1	Transmembrane protein 70	0.64	0.0044
FAM128A	BG332462	Family with sequence similarity 128, member A	0.63	0.0043
–	W87901	–	0.60	0.0047
CCDC85B	NM.006848.1	Coiled-coil domain containing 85B	0.59	0.0024
FAM131A	AI141670	Family with sequence similarity 131, member A	0.53	0.0023
–	AI201594	MRNA; cDNA DKFZp762M127 (from clone DKFZp762M127)	0.42	0.0029

stored under ethanol and finally hybridized for 15–20 h in hybridization buffer [50% deionized formamide/10% (v/v) dextran sulphate (50%)/0.3 M NaCl/30 mM Tris/HCl (pH 7.4)/4 mM EDTA/1 × Denhardt's/0.5 mg/ml polyadenylic acid/0.5 mg/ml denatured salmon sperm DNA] containing the radiolabelled probe with a specific radioactivity of 3500 c.p.m./ μ l. The labelled oligonucleotide probes were generated with terminal transferase by using [35 S] dATP α S (Amersham, England, UK). Anti-sense oligonucleotides used for LDB2, NELL2 and protein kinase C β -1 (PRKCB1) are presented in Supplementary Table S3. Optimal oligonucleotide sequences (45-mers, 50–60% GC, low hairpin and dimer formation probability) were selected by using Oligo 5.0 (NBI, Plymouth, MN, USA). Hybridizations with a 1000-fold excess of the respective unlabelled oligonucleotide served as negative controls. After hybridization, sections were washed twice with 1 × saline-sodium citrate (SSC)/0.1% (v/v) 2-mercaptoethanol at room temperature for 20 min, once with 1 × SSC/0.1% (v/v) 2-mercaptoethanol at 57°C for 45 min, once with 1 × SSC at room temperature for 5 min and once with 0.1 × SSC at room temperature for 2 min. Sections were then

dehydrated, air-dried and exposed to Kodak BioMax film (Eastman Kodak, NewHaven, CT, USA) for 2 weeks at room temperature. Slides were dipped in photographic emulsion (Kodak NTB3; Eastman Kodak), incubated for 6–9 weeks and developed in Kodak D-19 developer (Eastman Kodak) for 3.5 min. For analysis with bright-field optics and to confirm cytoarchitecture, sections were counterstained with cresyl violet.

Plasmid construction

The vector pSuper.neo+gfp (VEC PBS 0006, Oligoengine, Seattle, USA) was used for shRNA studies. The procedure for preparing constructs coding for shRNA was described previously (Brummelkamp *et al.*, 2002). The gene-specific targeting sequence (19 nt) separated by a short spacer from the reverse complement of the same sequence and five thymidines (T5) as termination signal was subcloned (for detailed information see Supplementary Material). The specific murine target sequence for LDB2 was designated shRNA-mLDB2 and the human control shRNA for

LDB2 was designated shRNA-hLDB2. Sequences were confirmed by NCBI Blast and had no homology with any other vertebrate genes (Supplementary Tables S4 and S5). The full-length mLDB2 (NCBI accession number NM_010698) was cloned by PCR, with sense primer 5'-GCG AGA TCT CCA AGA TGT CCA GCA CAC CA-3' (BglII restriction site) and an antisense primer 5'-GCG GTC GAC TCT GGG AAG CCT GGG GTG-3' (Sall restriction site) using RZPD clone (IRAKp961M10176Q2, BC079611) as template. The fragment was inserted into the mammalian expression vector pCMV-myc2 (generous gift of A. Maximov, Dallas, USA). The yellow fluorescent protein from the pVenus vector (generously provided by M. Schwarz, Heidelberg, Germany) was also cloned by PCR with the sense primer 5'-GCG GTC GAC AAG TGA GCA AGG GCG AGG AG-3' (Sall restriction site) and the antisense primer 5'-GCG GGA TCC ATT ACT TGT ACA GCT CGT CCA TGC-3' (BamHI restriction site). The vector pCherry (generously provided by T. Sudhof, Dallas, USA) encodes for a red fluorescent protein, which was co-transfected when using the vector pCMV-myc2-mLDB2-Venus. The obtained vectors were subsequently sequenced to verify the integrity of the fusion protein. pGUR-shGFP was kindly provided by B. Sabatini (Boston, USA).

Western blot analysis

Equal amounts of protein extracts (20 µg/sample) from transfected 293T cells were separated by SDS-PAGE and blotted to nitrocellulose over night (45 mA). After blocking with 5% skim milk solution and 5% fetal calf serum, membranes were incubated with mouse anti-β-actin for control and rabbit polyclonal anti-green fluorescent protein (anti-GFP) antibodies followed by decoration with peroxidase labelled anti-mouse or anti-rabbit IgG, respectively. The bound complexes were detected with the ECL-detection system (Amersham Pharmacia biotech, UK).

Neuron culture and transfection

Primary hippocampal neuron cultures were prepared from embryonic day 19 (E19) mouse brains (Banker and Goslin, 1998). Cells were plated on poly-D-lysine coated (0.01%) in 24-well plates at a density of 150 000 cells/well. Hippocampal cultures were grown in Basal Medium Eagle (BME; Invitrogen, Carlsbad, CA, USA) supplemented with 2% B27 (Invitrogen), 1% glucose (Invitrogen) and 1% fetal calf serum (Invitrogen). At 5 d *in vitro* (DIV) hippocampal neurons were transfected using 1 µl lipofectamine 2000 and 1 µg plasmid DNA/well for 3 h. The cells were washed twice with supplemented BME and the original medium was transferred back on the cells. In case of co-transfection, the DNA of interest was labelled with GFP and mixed with pCherry in a 1:0.3 ratio.

Image analysis and quantification

Digital images of single transfected neurons (at high magnification, ×400) were subjected to morphometric analyses and quantification using ImageJ software (Wayne Rasband, NIH, MD, USA). For measurements of primary, secondary and tertiary dendrites, each branch was traced from branching point to the tip, and the number of pixels was automatically calculated. All quantifications were performed by investigators 'blind' to the experimental condition. Data were obtained from three independent neuronal preparations and transfections and in each

transfection three wells were transfected with the identical combination of plasmids.

Results

This comprehensive gene expression analysis of gangliogliomas including the neuropathological spectrum of architectures presented in Fig. 1 was performed from histologically verified tumour as well as adjacent normal brain tissue, both matched for equal amounts of grey and white matter. All microarray hybridizations were subjected to quality assessment and fulfilled technical requirements for reliable data mining strategies. The full array data set will be available on ArrayExpress ('gangliogliomas'; <http://www.ebi.ac.uk/microarray-as/ae/>). Statistically more than one-third of the transcripts were assigned 'present'. The average background signal was 67 compared to an average signal genes designated present (338), marginal (85) or absent (32). Comparative data mining between tumour and control tissue was performed by R (V.1.9.1). Pairwise Q-Q plots were used to address the data integrity. All Q-Q plots aligned well along the main diagonal, confirming the comparability of the expression distributions across different samples (Fig. 2A). Established normalization and pre-filtering procedures diminished false positive low-abundant transcripts.

Subsequently, we have carried out different clustering approaches to the data. Unsupervised cluster analysis based on large sets of expression data provides information on the global effects that differentiate samples under study (Brehelin *et al.*, 2008). In this respect, we performed cluster analysis with all present genes based on euclidean distance as a sample-wise distance measure and average linkage as a set-wise distance measure. This analysis demonstrated tumours and controls to be fairly well separated (Fig. 2B). Intriguingly, in the euclidean distance matrix only Patients 3 and 5 had their respective tumour and control samples closest to each other. These data suggest, that even in highly differentiated tumours such as gangliogliomas, the parameter 'tumour' appears to be generally more distinctive than 'identical genetic background' with respect to gene expression patterns. We excluded contamination effects between tumour and control tissue to be the cause of close sampling between samples of Patients 3 and 5.

Although it needs to be emphasized that there is no gold standard for 2-way hierarchical cluster analyses of large-scale gene expression data, it is useful as an explorative tool displaying the predominant differences across samples, together with the genes that are best suited to differentiate between them (Raychaudhuri *et al.*, 2001). Using a paired *t*-test followed by Benjamini-Hochberg correction for multiple testing, we observed 94 transcripts to be differentially expressed between gangliogliomas and controls. These transcripts fulfilled several stringent criteria, i.e. expression higher than the normalized median and a two-sided fold-change of at least 1.5 between gangliogliomas

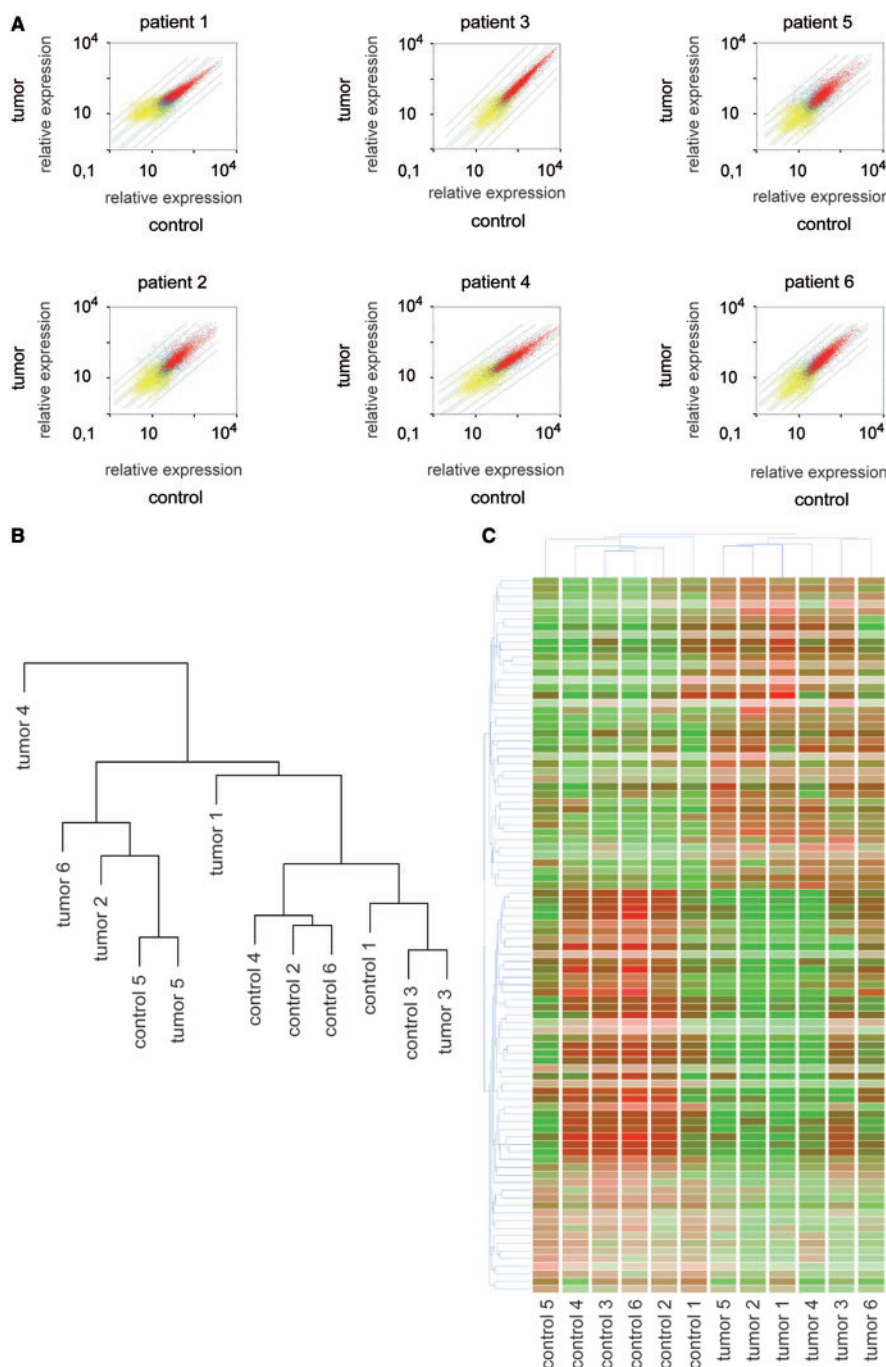


Fig. 2 Oligonucleotide array analysis in gangliogliomas. **(A)** Scatterplot analysis of individual tumour-control pairs to monitor the data quality. The distribution of the datapairs around the main diagonal suggests the absence of systematic effects favouring one of the two control- or tumour sample group (control = y-axis; tumour = x-axis). Logarithmic plot of the intensity scores, as obtained from the Affymetrix software, after standard normalization are presented as relative expression values based on Affymetrix light units. **(B)** Result of unsupervised hierarchical clustering based on all present genes using euclidean distance as a sample-wise distance measure and average linkage as a set-wise distance measure. Unsupervised cluster analysis based on such large sets of expression data provides information on the most relevant parameter that differentiates samples under study (Brehelin *et al.*, 2008). In the present analysis, this parameter is clearly given by the parameter 'control' and 'tumour', although for Patients 3 and 5, tumour and control samples have closest distance to each other (see main text for further discussion on this aspect). **(C)** Hierarchical clustering of 94 differentially expressed genes between gangliogliomas and control brain tissue (distance measure = Euclidean distance; clustering method = average linkage). The hierarchical clustering method generates a dendrogram in which closely related samples have a short distance from each other in the dendrogram. The first six columns represent individual control tissue data and the second six columns tumour tissue data, respectively. Each row of coloured boxes represents expression of one gene. Colours indicate relative gene expression levels, with red representing abundant expression and green representing reduced expression levels compared to mean expression of the respective gene. Note, that clusters of genes, which are abundant in gangliogliomas are low in expression in controls and vice versa.

and controls. These data mining settings allowed to detect particularly transcripts with both stable and relevant expression alterations. These 94 transcripts are significantly differentially expressed between gangliogliomas and controls (Table 1). Nevertheless, we observed a certain amount of variability in expression between different gangliogliomas (Fig. 2C). This feature may partly reflect the cellular spectrum within and between gangliogliomas (Becker *et al.*, 2007). By clustering genes based on similar expression patterns hierarchically into nearby places we obtained a condition genetree (Fig. 2C). This analysis revealed two large clusters of transcripts that showed either high levels of expression in controls and low abundance in gangliogliomas or vice versa.

In order to validate the differential gene expression data from the array experiments described above, we used real-time RT-PCR and concentrated on representative transcripts from the low-, intermediate- and high copy range in gangliogliomas and controls. In parallel to this aspect and similarly to previous array analyses of brain disorders (Gorter *et al.*, 2006; Kang *et al.*, 2007), in these verification analyses we followed transcripts with a potential relevance to pathogenetic processes as discussed in detail subsequently. Expression levels were determined in duplicates and normalized to the reference gene β -actin by the $\Delta\Delta C_t$ method (Chen *et al.*, 2001). Tribbles homolog 1 (TRIB1) and ST6GalNAc4 as low copy transcripts, NELL2, PRKCB1 and LDB2 as intermediate abundant mRNAs and AI201594, heat shock 40 kDa protein 4 (HSJ2) as well as ADP-ribosylation factor 3 (ARF3) as high copy genes confirmed expression differences between gangliogliomas and controls previously observed by expression arrays (Fig. 3). Furthermore, we used *in situ* hybridization to resolve differential transcript expression of several of these transcripts between glial and neuronal components of gangliogliomas (Fig. 4). In order to compare gene expression in gangliogliomas with the second major entity of epilepsy-associated glioneuronal neoplasms, we carried out real-time RT-PCR for the transcripts addressed before in gangliogliomas also in DNETs (Fig. 5).

The set of 94 differentially expressed genes in gangliogliomas (Fig. 2) was subjected to a gene ontology analysis (NetAffx-Portal). Differential expression of more than individual genes related to a circumscribed number of elementary cellular functions and molecular pathways as follows (Table 1).

Regulation of chromatin state and transcription factors

Gangliogliomas are characterized by dysplastic, often binuclear neuronal components and proliferation active glial cells (Blümcke *et al.*, 1999). These neuropathological characteristics are reflected by chromosomal aberrations in the distinct cellular components (Hoischen *et al.*, 2008)

and may relate to aberrant transcriptional control. The chromodomain-protein coding gene CDY1 is strongly reduced in expression in gangliogliomas, which can contribute to impaired chromatin assembly since several chromodomain-proteins have been reported as tumour suppressors that are important for chromatin rearrangement. Further, impaired function of chromodomain-proteins underlies defects in developing tissues (Bagchi *et al.*, 2007; Hurd *et al.*, 2007). The B-cell CLL/lymphoma 11A (Bcl11A) gene that encodes for a Kruppel-like zinc-finger protein, has been shown to be relevant for B-cell development and is abundantly expressed in brain (Kuo and Hsueh, 2007). Reduced expression of Bcl11A in gangliogliomas may be associated with the lack of maturation in its cellular components. Modified nuclear gene activation patterns have substantial consequences for several cellular functions, which are mediated by altered intracellular signalling.

Intracellular signal transduction

Expression of multiple genes involved in intracellular signalling was altered in gangliogliomas. The differentially expressed genes were associated with distinct cellular compartments. Expression array and real-time RT-PCR data showed that HSJ2, a co-chaperone of Hsc70 was lower in expression in gangliogliomas as compared to controls. HSJ2 has been suggested to play a role in protein import into mitochondria (Oh *et al.*, 1993; Kanazawa *et al.*, 1997). Impairment of mitochondria function and mitochondrial DNA damage have been reported in the course of epileptic seizures (Baron *et al.*, 2007). Accordingly, this differential expression is not restricted to gangliogliomas but also present in DNETs (Fig. 5). ARF3 is a GTP-binding protein involved in protein trafficking that may modulate vesicle budding and uncoating within the Golgi apparatus (Tsai *et al.*, 1991; Takeya *et al.*, 2000). It is strongly up-regulated in mantle zone during brain development (Takeya *et al.*, 2000). ARF3 mRNA levels are lower in gangliogliomas than in controls (Table 1, Fig. 3). This finding may relate to aberrant protein trafficking and irregular migration not only of ganglioglioma but also DNET cell components (Fig. 5).

A further interesting class of molecules altered in astrocytic tumour cells as well as under epileptic conditions is related to ganglioside biosynthesis (Yu *et al.*, 1987; Abate *et al.*, 2006). α -N-acetyl-neuraminyl-2,3- β -galactosyl-1,3-N-acetyl-galactosaminide α -2,6-sialyltransferase (ST6GalNAc4) is substantially reduced in expression in gangliogliomas (Table 1, Fig. 3; Harduin-Lepers *et al.*, 2000). It belongs to the glycosyltransferase 29 family and is involved in the biosynthesis of ganglioside GD1A from GM1B (Harduin-Lepers *et al.*, 2000). Recent data from astrocytoma cell lines have suggested that reduced presence of gangliosides including GD1A relates to a less invasive biological behaviour with respect to growth and vascularization

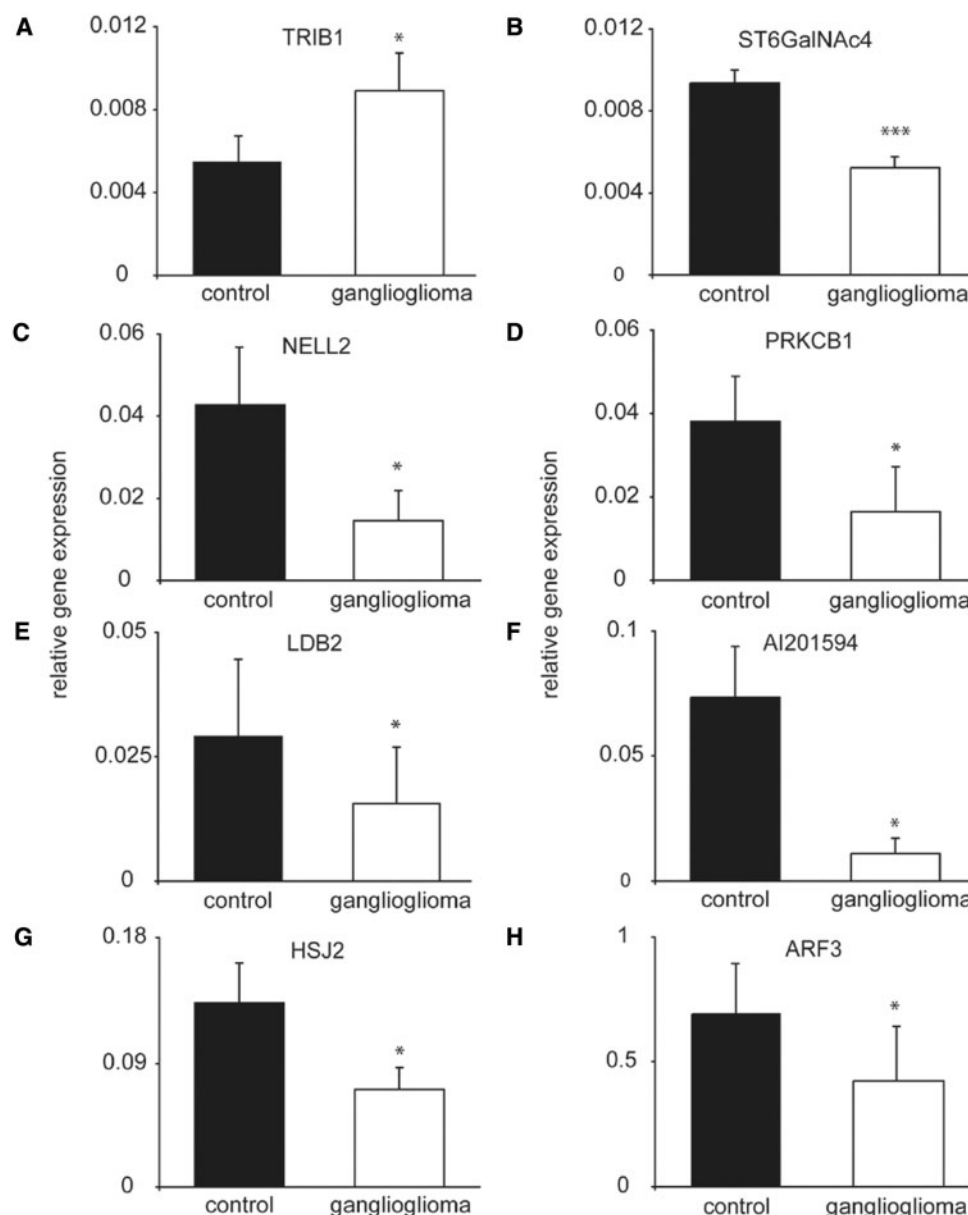


Fig. 3 Real-time qRT-PCR of low-, intermediate- and high copy transcripts differentially expressed between gangliogliomas and controls. **(A)** TRIB1 represents a low-abundant transcript whose expression was observed to be increased in gangliogliomas on the arrays. This finding is confirmed by real-time RT-PCR. **(B)** The low copy mRNA ST6GalNAc4 is reduced in expression in gangliogliomas as previously observed by gene array analysis. Real-time RT-PCRs for the intermediate copy transcripts NELL2, PRKCB1 and LDB2 **(C–E)** as well as the high copy mRNAs AI201594, HSJ2 and ARF3 **(F–H)** confirms expression differences observed by expression arrays. AI201594 is an expressed sequence tag (EST) partially similar to β -arrestin I, which regulates β -adrenergic receptor function (Parruti et al., 1993). β -Arrestins bind phosphorylated β -adrenergic receptors, thereby causing a significant impairment of their capacity to activate G proteins that can be involved in aberrant signalling cascades in gangliogliomas. Due to the fact that AI201594 represents an EST, it has been grouped as 'varia' (Table I). Pathogenetic implications of differential expression of the other transcripts analysed by real-time qRT-PCR in gangliogliomas are discussed in the main text. Expression levels were determined in duplicates and normalized to the reference gene β -actin by the $\Delta\Delta C_t$ method. The error bars represent SEM ($n = 6$ each for gangliogliomas and controls; t -test: * $P < 0.05$, *** $P < 0.001$).

stimuli of tumour cells (Abate *et al.*, 2006). Low expression of ST6GalNAc4 in gangliogliomas is well compatible with this benign phenotype. Remarkably, altered expression of ST6GalNAc4 is not present in DNETs, which are characterized by a fundamentally different, multilocular growth pattern (Fig. 5).

Several differentially expressed transcripts such as the inositol 1,4,5-trisphosphate 3-kinase B, the protein kinase C ι , AKT3 and the Rho-type GTPase-activating protein RICH2 (Table 1) point towards further alterations within phosphatidylinositol 3-kinase pathway signalling in gangliogliomas (Schick *et al.*, 2007b). The phosphatidylinositol

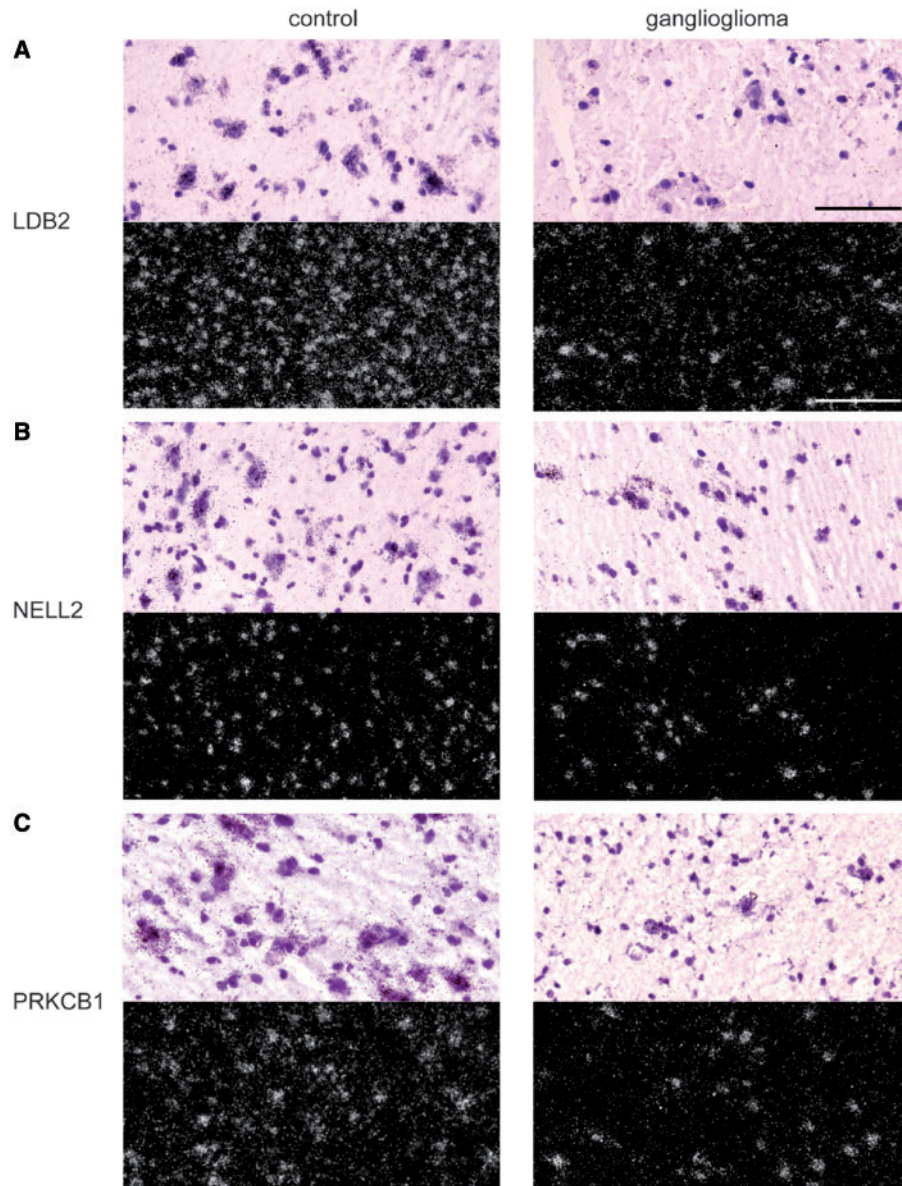


Fig. 4 Cellular resolution of differentially expressed genes by radioactive *in situ* hybridization. Microscopic bright- (top) and dark-field (bottom) images show the distribution of LDB2 (**A**), NELL2 (**B**) and PRKCB1 (**C**) mRNA in representative control versus ganglioglioma tissue. Brain sections were hybridized with ^{35}S -labelled oligonucleotides specific for LDB2, NELL2 or PRKCB1. Neurons as well as glial cells are present in control and ganglioglioma tissue samples. Neuronal cells can be differentiated by larger nuclei (bright field). Note the lower expression of NELL2, PRKCB1 and LDB2 in neuronal cell components of gangliogliomas versus controls (dark field). Negative controls with excess of unlabelled oligonucleotides were devoid of signal (data not shown; magnification and scale bars: bright field: $\times 200$, $100\text{ }\mu\text{m}$; dark field: $\times 40$, $500\text{ }\mu\text{m}$).

3-kinase signalling pathway is critically involved in the development of malformative dysplastic precursor lesions as well as gangliogliomas (Schick *et al.*, 2006; Schick *et al.*, 2007a). Expression of PRKCB1 is substantially reduced in gangliogliomas as demonstrated by expression array and real-time qRT-PCR data (Figs 2 and 3). Furthermore, *in situ* hybridization analysis suggested that PRKCB1 is reduced in small glial as well as dysplastic neuronal cell elements in gangliogliomas (Fig. 4). PRKCB1 is a calcium-activated, phospholipid-dependent, serine- and

threonine-specific enzyme. PRKCB1 is activated by diacylglycerol, and in turn phosphorylates a range of cellular proteins. Protein Kinase C (PKC) also serves as the receptor for phorbol esters, a class of tumour promoters (Niino *et al.*, 1992). Induction of several PKC isoforms has been reported after epileptic seizures promoting glutamate-mediated cell death (McNamara *et al.*, 1999). Lower expression of PRKCB1 in gangliogliomas may antagonize seizure-induced cell death in these tumours an aspect that is potentially shared by DNETs (Fig. 5).

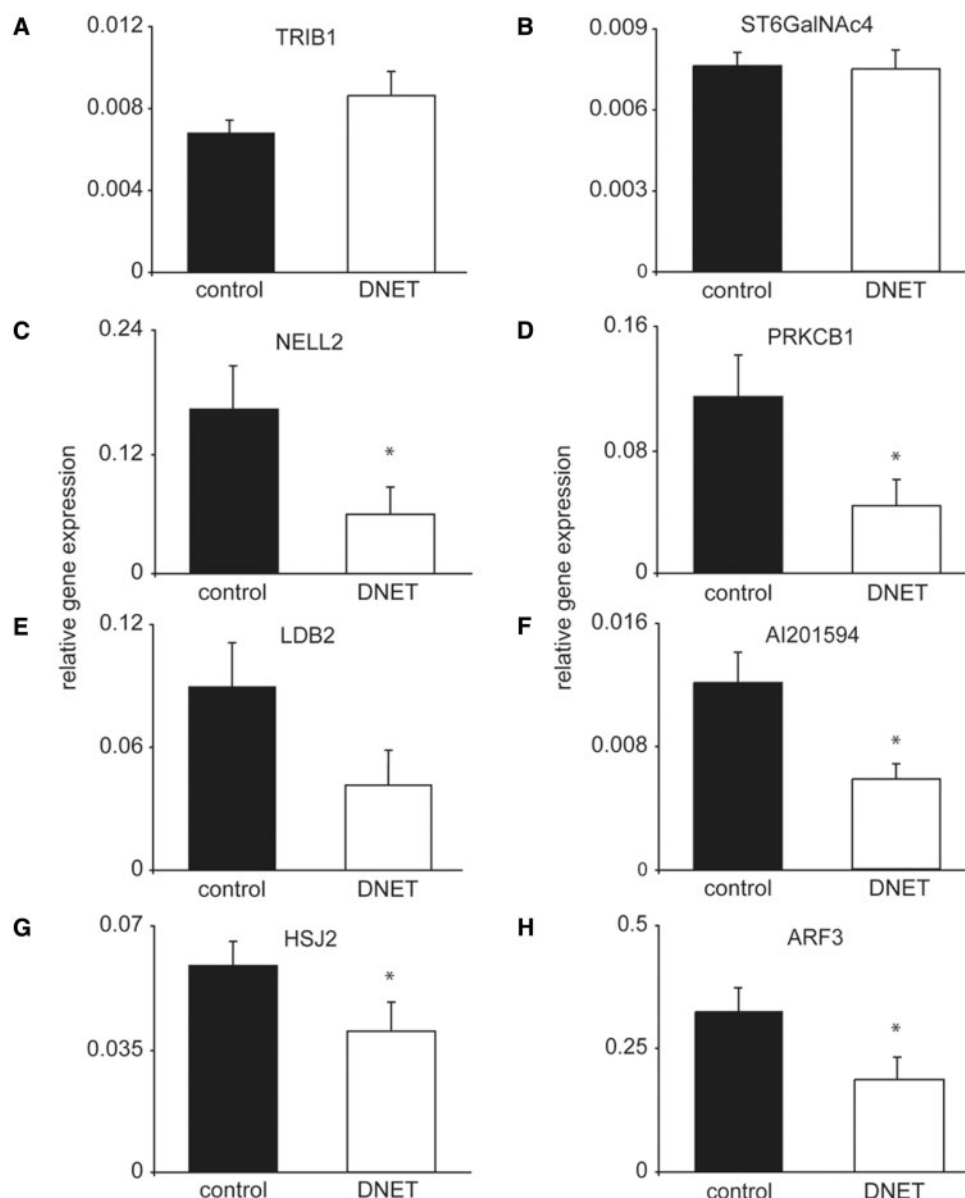


Fig. 5 Real-time qRT-PCR between DNETs and controls. *NELL2*, *PRKCB1*, *AI201594*, *HSJ2* and *ARF3* are significantly reduced in expression in DNETs compared to control brain tissue of the same patients (**C**, **D**, **F**, **G** and **H**). In contrast, no significant differences in transcript abundance are observed for *TRIB1*, *LDB2* and *ST6GalNAc4* between DNETs and controls (**A**, **B**, and **E**). Expression levels were determined in duplicates and normalized to the reference gene β -actin by the $\Delta\Delta C_t$ method. The error bars represent SEM ($n = 7$ each for DNETs and controls; t -test: $*P < 0.05$).

Transduction of extracellular signals and cell adhesion

mRNA levels of the protein kinase C-binding protein *NELL2* are also lower in gangliogliomas as well as DNETs (Table 1, Figs 3 and 5) (Watanabe *et al.*, 1996). *In situ* hybridization revealed a similar cellular pattern of reduced expression for *NELL2* in gangliogliomas compared to controls as observed for *PRKCB1* (Fig. 4). Impaired expression of *NELL2* in gangliogliomas can contribute to aberrant cellular positioning and differentiation in glioneuronal tumours (Nelson *et al.*, 2004).

Compared to diffusely infiltrating astrocytomas as well as to highly circumscribed, i.e. pilocytic astrocytomas, gangliogliomas can present with an intermediate infiltrating growth pattern. This biological feature may be reflected by increased expression of only individual extracellular matrix proteases, i.e. the matrix metalloproteinase 2 (MMP2) and tissue plasminogen activator (PLAT) (Landau *et al.*, 1994; Fillmore *et al.*, 2001). Abundant expression of these genes reflects the moderate invasive growth character of gangliogliomas, by which these glioneuronal tumours differ from the more frequent diffusely infiltrating glial brain tumours as well as by their low-proliferation activity.

Control of cell cycle and proliferation

Cell cycle activity and proliferation of gangliogliomas are generally low; however, regulation of cell cycle and proliferation of cellular components certainly constitute general key features of tumour growth. Considering a central aspect of ganglioglioma development, i.e. neoplastic transformation of the glial component from pre-existing dysplastic precursor lesions, impaired cell cycle control and increased proliferation are critical for tumourigenesis. A lower overall neuronal density recently observed in cortical dysplasias suggested as precursor lesions for gangliogliomas relates to inadequate local proliferation or secondary degeneration of neural precursors (Thom *et al.*, 2005). Aberrant expression of cell growth and apoptosis-associated genes and proteins has been reported in cortical dysplasias as well as in gangliogliomas (Prayson, 1999; Kim *et al.*, 2003). TP53-inducible protein 3, abundantly expressed in gangliogliomas has been found to impair cell cycle regulation (Nicholls *et al.*, 2004), and can be involved in aberrant growth control in gangliogliomas. In the ganglioglioma series under study, only individual cellular ganglioglioma components accumulate the TP53 protein, not suggesting a mutation of the underlying gene (data not shown). TP53-inducible protein 3 has not been reported to be abundantly expressed in other low-grade brain tumours such as diffuse astrocytomas (WHO grade II) or pilocytic astrocytomas.

TRIB1 transcripts are almost 2-fold induced in gangliogliomas as compared to controls, which was also confirmed by qRT-PCR (Table 1, Fig. 3). Interestingly, this up-regulation is not observed in DNETs (Fig. 5). TRIB1 interacts with and regulates activation of MAP kinases (Kiss-Toth *et al.*, 2004). The MAP kinase pathway is centrally involved in cellular differentiation, growth and programmed cell death, characteristics which are substantially disturbed in gangliogliomas and may contribute to aberrant proliferation as well as differentiation of glial and neuronal components in gangliogliomas.

Development and differentiation

Cytological and histological characteristics suggest compromised differentiation of neuronal precursors during cortex development to play a role in gangliogliomas (Schwartzkroin and Walsh, 2000; Golden, 2001; Bentivoglio *et al.*, 2003). In the present expression array data set, several differentially expressed genes relate to the development of the central nervous system and the differentiation of neural precursor cells. Of this group, the most abundant transcript in gangliogliomas is the nerve growth factor receptor (NGFR, p75) (Tapia-Arancibia *et al.*, 2004). Whereas, neurotrophins such as brain-derived neurotrophic factor (BDNF) were observed increased in expression in the neuronal ganglioglioma components, increased p75 was reported in reactive microglia cell components within gangliogliomas (Aronica *et al.*, 2001; Aronica *et al.*, 2004).

LIM domain-containing proteins constitute important regulators that determine cellular fate and differentiation during embryogenesis (Dawid *et al.*, 1998). Here, we observed two LIM domain-interacting transcripts, i.e. LIM domain only 4 (LMO4) and LDB2, to be substantially lower in expression in gangliogliomas as compared to controls (Table 1). Reduced expression of LMO4 in gangliogliomas reflects the benign biological behaviour of gangliogliomas in contrast to malignant neuroblastic tumours (Aoyama *et al.*, 2005). LDB2 binds the LIM domain of two families of transcription factors, LIM-homeodomain proteins (LIM-HD) and LIM-only proteins (LMO). It has been recently shown that the interaction of LDBs with LIM domains is critical for the development of neurons (Fernandez-Funez *et al.*, 1998). LIM-HD transcription factors are substantially expressed in neurons and essential for neuronal development (Lundgren *et al.*, 1995; Pfaff *et al.*, 1996; Benveniste *et al.*, 1998; Way and Chalfie, 1988). LDB2 is significantly reduced in expression in gangliogliomas (Table 1, Fig. 3). The overall expression level of LDB2 in gangliogliomas is remarkably higher than in DNETs (Figs. 3 and 5). Furthermore, we did not observe a significant down-regulation of LDB2 mRNA in DNETs as compared to controls, although a certain tendency in this direction could be detected (Fig. 5). By *in situ* hybridization, we demonstrated that reduced expression of LDB2 mRNA is present in dysplastic, clustered neuronal components but not in glial cell elements of gangliogliomas (Fig. 4).

Considering the unique neuropathological aspect of gangliogliomas, i.e. dysplastic and immature neuronal cell components, we focused our further analysis on the functional role of LDB2 for neuronal development. To this end, we applied an shRNA approach to selectively knock-down the expression of murine LDB2 in primary hippocampal cells. We first tested the efficiency and the specificity of the knock-down in HEK293T cells that had been co-transfected with plasmids encoding a LDB2-eGFP fusion protein and an shRNA targeted against murine LDB2 (shRNA-mLDB2). Levels of the LDB2-eGFP fusion protein were reduced by 80% 120 h after transfection (Fig. 6A and B). Using the same assay, an shRNA against the human LDB2 homologue (shRNA-hLDB2) did not result in a significant knock-down of LDB2-eGFP even though there is a sequence homology of >98% between murine and human LDB2 cDNAs (Fig. 6A and B). In the subsequent experiments, shRNA-hLDB2 and an unspecific shRNA against GFP (pGUR-shGFP) were therefore used to control for off-target effects. We then transfected primary hippocampal neurons with the plasmid encoding the shRNA against murine LDB2 and the control plasmids pSuper, shRNA-hLDB2 and pGUR-shGFP (Fig. 6C–F). Transfection of primary hippocampal neurons with the plasmid encoding pCMV-LDB2, i.e. resulting in over-expression of LDB2, did not result in significant morphological differences as compared to controls (data not shown). Whereas, native primary hippocampal neurons

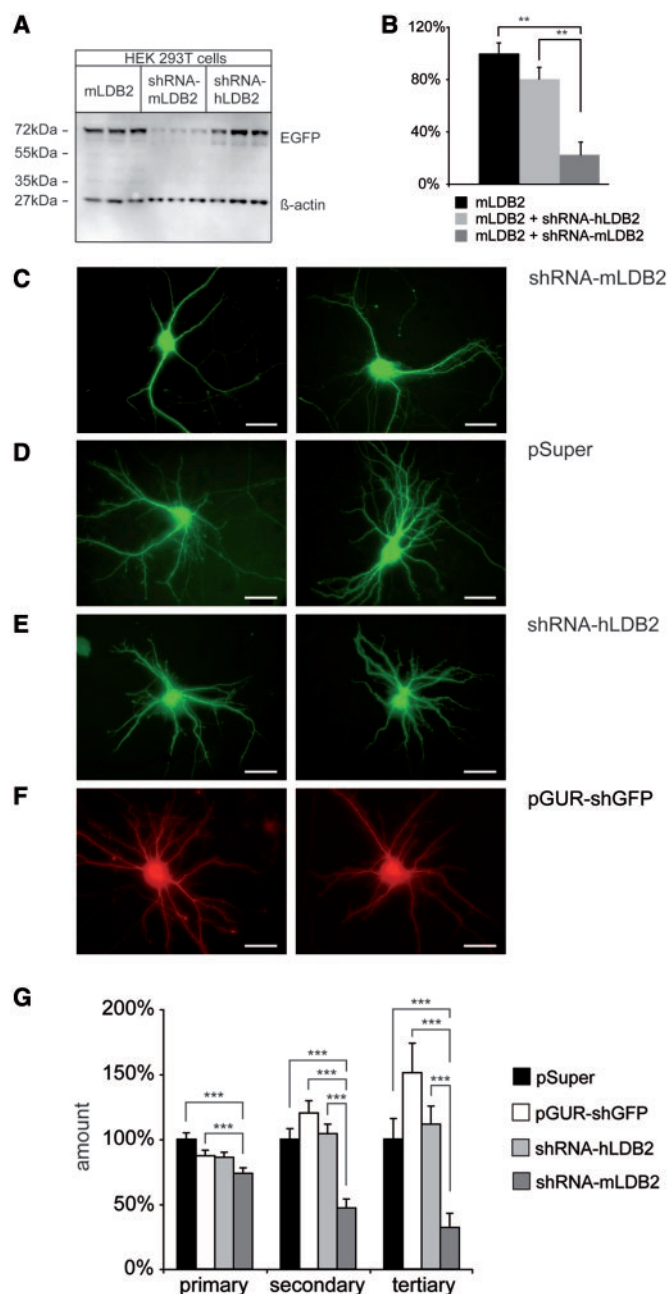


Fig. 6 (A, B) Analysis of the silencing efficiency and specificity of an shRNA targeted against murine LDB2. (A) HEK293T cells were transfected with pCMV-mLDB2-Venus and co-transfected with shRNA-mLDB2 and shRNA-hLDB2. Total cell lysates were prepared, and equal lysates fractions (20 μ g/lane) were analysed by immunoblotting. The blot was probed with antibodies against EGFP and β -actin. Numbers on the left indicate positions of molecular weight markers. Only the shRNA targeted against the murine LDB2 but not the one against the human LDB2 results in an efficient knock-down of murine LDB2. (B) Quantification of the knock-down efficacy of the shRNA-vectors was performed with the AIDA software. Transfection with shRNA-mLDB2 reduced the expression of LDB2 up to 80%; whereas, the shRNA against human LDB2 did not significantly reduce LDB2 expression and was therefore used as control in the following experiments. The error bars represent SEM (t-test: $^{**}P < 0.005$). (C–F) LDB2 promotes dendritic branching of developing hippocampal neurons.

showed a densely arborized pattern of processes, neurons with reduced expression of LDB2 revealed substantial structural impairment, i.e. aberrant arborization. These alterations are absent in all control conditions (Fig. 6C–F). Quantitatively, we observed a substantial reduction of the amount of dendrites reflecting the complexity of the dendritic tree in primary hippocampal neurons transfected with shRNA-mLDB2. This alteration affected the distal, tertiary dendritic compartment but also primary and secondary dendrites (Fig. 6G). LDB2 and its interacting partners represent a novel family of molecules potentially involved in aberrant development of ganglioglioma components.

Discussion

Gangliogliomas are complex glioneuronal brain tumours frequently associated with pharmacoresistant epilepsies. Gene expression studies using microarrays allow a comprehensive analysis of transcript alterations that reflect pathomechanisms operating in gangliogliomas. By using a stringent clustering approach, we have observed 94 transcripts to be differentially expressed between gangliogliomas and control tissue. Generally, such alterations of gene expression are the consequence of modified epigenetic regulation and/or mutations of promoters that control gene expression. However, not only such factors intrinsic to ganglioglioma cell components but also the interaction of tumour elements with the environment including immune mechanisms, propensity for infiltration and, in functional regards, epileptogenicity influence the expression profile of these tumours. Some of the identified gene profiles are new; other results extend or confirm previous findings on gene expression alterations in gangliogliomas as outlined for individual gene clusters above. Here, we will focus on distinct aspects of gangliogliomas based on our microarray and subsequent analyses related to aberrant development of neuronal precursors and glial components as well as differences in expression profiles of gangliogliomas and other low-grade primary brain tumours.

Focal epilepsies constitute multifactorial disorders (Elger, 2002). The pathogenesis of focal epileptic attacks is not entirely understood and the relative contribution to

Representative confocal images of primary hippocampal neurons at DIVII that had been transfected at DIV5. (C) Substantial morphological impairment of dendritic arborization was present in hippocampal neurons transfected with shRNA-mLDB2. As control experiments, primary neurons were transfected with the control vectors pSuper D, shRNA-hLDB2 E and pGUR-shGFP (F, co-transfected with pCherry). Morphologically, neuronal cells exposed to control vectors showed dense dendritic branching. (G) LDB2 has substantial effects on dendritic branching in developing hippocampal neurons. The number of all primary, secondary and tertiary dendrites, in shRNA-mLDB2 transfected neurons was significantly reduced versus controls. Photographed cells were measured morphometrically with ImageJ. (black: pSuper; white: pGUR-shGFP; grey: shRNA-hLDB2; dark grey: shRNA-mLDB2; t-test: $^{***}P < 0.001$).

epileptogenicity of lesional versus perilesional areas is variable between individual patients (Wong, 2008), which limits the significance of differential gene expression patterns in this respect. Lesions can disrupt the anatomic architecture and conduction routes of the central nervous system. Seizures are elicited by deafferenting areas of the cerebral cortex or by immediate physical effects such as stretching of brain tissue, impairment of the extracellular space, altered homeostasis of neurotransmitter clearance as well as ion equilibrium, which contributes to aberrant synchronous discharges (Heinemann, 2004; Wolf *et al.*, 1995a; Binder and Steinhauser, 2006). In patients with electrically inert lesions such as glial scars and diffuse gliomas, these mechanisms will constitute the most likely scenario. Remarkably, although epileptic seizures are not infrequent in diffusely infiltrating gliomas, the frequency is much less than in glioneuronal tumours (Pace *et al.*, 1998).

In glioneuronal tumours and malformations, the population of dysplastic neuronal cells inherent to these lesions may actively participate in the generation of seizures in addition to the effects described above. This can be either through aberrant release of neurotransmitters or neuromodulators into the adjacent brain tissue or through the electrical activity of their intrinsic neuronal network (Wolf *et al.*, 1996; Cepeda *et al.*, 2007; Aronica *et al.*, 2008). The fact that epilepsy is substantially more frequent in gangliogliomas than in glial tumours argues for an active contribution of the neuronal component to epileptogenesis in these neoplasms. In addition, the interplay between lesional and surrounding tissue contributes to epileptogenesis, which constitutes an important factor for the outcome of epilepsy surgery (Wong, 2008).

Interestingly, it had been previously shown, that neurochemical profiles from ganglioglioma neuronal components are not substantially different from neurons in normal control CNS tissue (Wolf *et al.*, 1995b), and also in the present microarray analysis we do not observe numerous expression changes of neurotransmitter receptors or ion channels in gangliogliomas. Dysplastic neurons substantially contribute to aberrant signal transmission within the neuronal network (Knafo *et al.*, 2001). Many differentially expressed transcripts observed in the present study relate to aberrant differentiation of neuronal ganglioglioma components (Table 1, Figs 3 and 4). These dysplastic neuronal cells may contribute to an epileptogenic network, which in individual patients is not limited to the lesion but extends to the perilesional area. However, e.g. our LDB2 quantitative transcript analyses and *in situ* hybridization demonstrate a selectively reduced presence in neuronal ganglioglioma components, putatively contributing to their dysplastic differentiation. Our observation that neurons with reduced levels of LDB2 exhibit an altered morphological phenotype, characterized by a decrease in dendrite density, is the first functional evidence linking LDB2 to the molecular mechanisms underlying impaired development of a regular cortical architecture. Since

neuronal migration and differentiation processes rely on intercellular signalling (Wu *et al.*, 1999; Williams and Truman, 2004), a reduced dendrite density of developing neurons with silenced LDB2 during development of the brain may contribute to an abnormal neuronal network. Clearly, such individual alterations do not constitute factors sufficient to elicit epileptic attacks. Further alterations are required to manifest epileptic seizures such as growth of a neoplastic glial component and the interaction with perilesional factors and e.g. invading immune cells (Wong, 2008). Remarkably, many patients with glioneuronal tumours do not manifest epilepsy in early childhood but acquire seizures later in life. This may reflect glioneuronal tumours to constitute highly dynamic entities, which at a certain point overcome a virtual threshold to manifest seizures.

As described here, gangliogliomas have rather specific anatomical and clinical features. Does the microarray data argue for molecular neuropathological mechanisms in gangliogliomas distinct from other low-grade brain lesions? A variety of studies using expression microarray approaches have been conducted in cortical malformations as well as low-grade glial and glioneuronal tumours. Certainly, microarray data obtained from different sources may only be compared with great caution since substantial variability in the studies can contaminate the comparisons and differences with respect to factors such as the array platform used, the detection thresholds, control tissue, linear dynamic range of the arrays, etc. have considerable influence on the data.

In cortical dysplasias, distinct transcriptional profiles were found as compared to our present data (Kim *et al.*, 2003). A remarkable finding of this study was a substantially increased expression of anti-apoptotic elements and decreased expression of pro-apoptotic factors. Considering that we did not observe substantial overlap between differential gene expression in gangliogliomas of our collective and the reported expression profile in cortical dysplasias, the data suggest different molecular pathways to operate in both lesions. Whether the cortical dysplasias analysed by Kim and colleagues (2003) can constitute precursor lesions for gangliogliomas remains unresolved, since the group of cortical dysplasias analysed there is heterogeneous.

With respect to the literature as well as our present analysis, there are intriguing similarities as well as differences in expression patterns between gangliogliomas and DNETs. This may be particularly remarkable since DNETs show distinct neuropathological features, i.e. a composition of small oligodendroglia-like cell components as well as 'floating' neurons, which generally do not share the dysplastic features of neuronal ganglioglioma components (Daumas-Duport *et al.*, 2007). Increased presence of reactive microglia in gangliogliomas as well as DNETs has been interpreted as potential mechanism to contribute to epileptogenesis in glioneuronal tumours (Aronica *et al.*, 2005). We observed expression signals in the ganglioglioma

samples that may reflect microglia activation (Table 1). Furthermore, it was shown that DNETs share distinct features with gangliogliomas with respect to the expression of BDNF and TrkB (Aronica *et al.*, 2001).

Our present array analysis showed NGFR as the most abundant transcript in gangliogliomas. Tyrosine kinase receptors trkA, -B and -C were observed to be strongly expressed in neuronal components of gangliogliomas, FCD and DNET (Aronica *et al.*, 2004). Similarly, to these partially shared expression differences, our present data suggest gangliogliomas and DNETs to share some differential expression patterns (Figs 3 and 5), i.e. reduced expression of NELL2, PRKCB1, HSJ2 and ARF3. However, we identified several gene expression patterns that were specifically altered only in gangliogliomas such as for TRIB1, ST6GalNac4 and LDB2, related to distinct dysplastic features of these glioneuronal tumours.

Even though several studies have addressed gene expression using microarrays in gangliogliomas before, the experimental approaches applied were fundamentally different from ours and the potential for comparison is thereby limited. Clearly, gene expression data obtained from tissue specimens of gangliogliomas result in a mixed signal derived from glial and neuronal elements as well. We have here used *in situ* hybridization to resolve differential gene expression between these cell components. A more direct approach was recently taken by obtaining gene expression patterns from single ganglioglioma cell components (Samadani *et al.*, 2007). Nevertheless, substantial overlap is present with respect to gene groups and functional clusters differentially expressed in this analysis and our present data. Differential gene expression in dysplastic neurons strongly relates to the downstream component (mTOR) of the insulin receptor pathway (Samadani *et al.*, 2007). P75 NGF receptor which we found strongly up-regulated in our present set of gangliogliomas was reported to be substantially induced in expression in the astrocytic cell component of gangliogliomas (Samadani *et al.*, 2007). Another highly interesting aspect of ganglioglioma pathology has been recently highlighted by data obtained from microarrays using different detection algorithms as well as autopsy control tissue. This study suggested the presence of a substantial inflammatory and innate immune reaction in gangliogliomas (Aronica *et al.*, 2008). We also found microglia-related transcripts, e.g. CD14, to be induced in expression in gangliogliomas. It has been reported that CD14 mediates dendritic impairment by innate immune cells (Milatovic *et al.*, 2004), which may contribute to aberrant architecture of dysplastic neuronal components of gangliogliomas.

Our present data suggest substantially different molecules and pathways to be involved in ganglioglioma development as compared to low-grade diffusely infiltrating astrocytomas and pilocytic astrocytomas. Recent data showed the most prominent difference between diffusely and pilocytic astrocytomas related to induction of genes encoding

adhesion- and infiltration-related molecules in diffuse astrocytomas, well compatible with their specific growth pattern (Rorive *et al.*, 2006; Sharma *et al.*, 2007). Vice versa, a number of genes induced in pilocytic astrocytomas related to anti-migration, which is well compatible with the circumscribed growth pattern of pilocytic astrocytomas. Our analysis of gangliogliomas reveals an intermediate phenotype. Some transcripts related to invasions such as MMP2 and tissue plasminogen activator were induced in expression. This may reflect the generally only minor infiltration behaviour of gangliogliomas.

Taken together, the present study identifies new genes and molecular cascades to be differentially expressed in gangliogliomas as well as extends the knowledge on genes and pathways previously implicated in the pathogenesis of glioneuronal tumours. Particularly, it contributes to differentiate molecular cascades that play a role in distinct low-grade brain tumours and the aberrant differentiation of ganglioglioma cell components. Therefore, the present data provide a basis to develop functional models for glioneuronal tumours.

Acknowledgement

We thank B. Sabatini, M. Schwarz, T. Südhof and A. Maximov for plasmids.

Funding

Deutsche Forschungsgemeinschaft (SFB TR3, C6, B8 to A.J.B. and S.S., KForG 'Innate Immunity' TP2 to A.J.B. and Emmy Noether program to S.S.); Deutsche Krebshilfe (to J.F., M.M. and A.J.B.); Bundesministerium für Bildung und Forschung (NGFNplus to A.J.B. and S.S.); European Union EPICURE (to A.J.B.); the BONFOR program of the University of Bonn Medical Center (to A.J.B., M.M. and S.S.).

References

- Abate LE, Mukherjee P, Seyfried TN. Gene-linked shift in ganglioside distribution influences growth and vascularity in a mouse astrocytoma. *J Neurochem* 2006; 98: 1973–84.
- Aoyama M, Ozaki T, Inuzuka H, Tomotsune D, Hirato J, Okamoto Y, et al. LMO3 interacts with neuronal transcription factor, HEN2, and acts as an oncogene in neuroblastoma. *Cancer Res* 2005; 65: 4587–97.
- Aronica E, Boer K, Becker A, Redeker S, Spliet WG, van Rijen PC, et al. Gene expression profile analysis of epilepsy-associated gangliogliomas. *Neuroscience* 2008; 151: 272–92.
- Aronica E, Gorter JA, Redeker S, Ramkema M, Spliet WG, van Rijen PC, et al. Distribution, characterization and clinical significance of microglia in glioneuronal tumours from patients with chronic intractable epilepsy. *Neuropathol Appl Neurobiol* 2005; 31: 280–91.
- Aronica E, Leenstra S, Jansen GH, van Veelen CW, Yankaya B, Troost D. Expression of brain-derived neurotrophic factor and tyrosine kinase B receptor proteins in glioneuronal tumours from patients with intractable epilepsy: colocalization with N-methyl-D-aspartic acid receptor. *Acta Neuropathol* 2001; 101: 383–92.
- Aronica E, Ozbas-Gerceker F, Redeker S, Ramkema M, Spliet WG, van Rijen PC, et al. Expression and cellular distribution of high- and low-affinity neurotrophin receptors in malformations of cortical development. *Acta Neuropathol* 2004; 108: 422–34.

- Bagchi A, Papazoglu C, Wu Y, Capurso D, Brodt M, Francis D, et al. CHD5 is a tumour suppressor at human 1p36. *Cell* 2007; 128: 459–75.
- Ballman KV, Grill DE, Oberg AL, Therneau TM. Faster cyclic loess: normalizing RNA arrays via linear models. *Bioinformatics* 2004; 20: 2778–86.
- Banker G, Goslin K. *Culturing nerve cells*. Vol. 2. Cambridge, MA: MIT Press; 1998.
- Baron M, Kudin AP, Kunz WS. Mitochondrial dysfunction in neurodegenerative disorders. *Biochem Soc Trans* 2007; 35: 1228–31.
- Becker AJ, Blümcke I, Urbach H, Hans V, Majores M. Molecular neuropathology of epilepsy-associated glioneuronal malformations. *J Neuropathol Exp Neurol* 2006; 65: 99–108.
- Becker AJ, Chen J, Zien A, Sochivko D, Normann S, Schramm J, et al. Correlated stage- and subfield-associated hippocampal gene expression patterns in experimental and human temporal lobe epilepsy. *Eur J Neurosci* 2003; 18: 2792–802.
- Becker AJ, Figarella-Branger D, Wiestler OD, Blümcke I. Ganglioglioma and gangliocytoma. In: Louis DN, Ohgaki H, Wiestler OD, Cavenee WK, editors. *WHO classification of tumours of the central nervous system*. Lyon: IARC; 2007. p. 103–5.
- Bentivoglio M, Tassi L, Pech E, Costa C, Fabene PF, Spreafico R. Cortical development and focal cortical dysplasia. *Epileptic Disord* 2003; 5 (Suppl 2): 27–34.
- Benveniste RJ, Thor S, Thomas JB, Taghert PH. Cell type-specific regulation of the *Drosophila* FMRF-NH2 neuropeptide gene by Apterous, a LIM homeodomain transcription factor. *Development* 1998; 125: 4757–65.
- Binder DK, Steinhäuser C. Functional changes in astroglial cells in epilepsy. *Glia* 2006; 54: 358–68.
- Blümcke I, Giencke K, Wardelmann E, Beyenburg S, Kral T, Sarioglu N, et al. The CD34 epitope is expressed in neoplastic and malformative lesions associated with chronic, focal epilepsies. *Acta Neuropathol* 1999; 97: 481–90.
- Blümcke I, Thom M, Wiestler OD. Ammon's horn sclerosis: a maldevelopmental disorder associated with temporal lobe epilepsy. *Brain Pathol* 2002; 12: 199–211.
- Brehelin L, Gascuel O, Martin O. Using repeated measurements to validate hierarchical gene clusters. *Bioinformatics* 2008; 24: 682–88.
- Brummelkamp TR, Bernards R, Agami R. A system for stable expression of short interfering RNAs in mammalian cells. *Science* 2002; 296: 550–3.
- Cepeda C, Andre VM, Wu N, Yamazaki I, Uzgil B, Vinters HV, et al. Immature neurons and GABA networks may contribute to epileptogenesis in pediatric cortical dysplasia. *Epilepsia* 2007; 48 (Suppl 5): 79–85.
- Chen J, Sochivko D, Beck H, Marechal D, Wiestler OD, Becker AJ. Activity-induced expression of common reference genes in individual CNS neurons. *Lab Invest* 2001; 81: 913–16.
- Cheung VG, Spielman RS, Ewens KG, Weber TM, Morley M, Burdick JT. Mapping determinants of human gene expression by regional and genome-wide association. *Nature* 2005; 437: 1365–69.
- Crino PB, Becker AJ. Gene profiling in temporal lobe epilepsy tissue and dysplastic lesions. *Epilepsia* 2006; 47: 1608–16.
- Daumas-Duport C, Pietsch T, Hawkins C, Shankar SK. Dysembryoplastic neuroepithelial tumour. In: Louis DN, Ohgaki H, Wiestler OD, Cavenee WK, editors. *WHO classification of tumours of the central nervous system*. Lyon: IARC; 2007. p. 99–102.
- Dawid IB, Breen JJ, Toyama R. LIM domains: multiple roles as adapters and functional modifiers in protein interactions. *Trends Genet* 1998; 14: 156–62.
- Dudoit S, Yang YH, Callow MJ, Speed TP. Statistical methods for identifying differentially expressed genes in replicated cDNA microarray experiments. *Stat Sin* 2002; 12: 111–39.
- Elger CE. Epilepsy: disease and model to study human brain function. *Brain Pathol* 2002; 12: 193–98.
- Fassunke J, Majores M, Ullmann C, Elger CE, Schramm J, Wiestler OD, et al. In situ-RT and immunolaser microdissection for mRNA analysis of individual cells isolated from epilepsy-associated glioneuronal tumours. *Lab Invest* 2004; 84: 1520–25.
- Fernandez-Funez P, Lu CH, Rincon-Limas DE, Garcia-Bellido A, Botas J. The relative expression amounts of apterous and its co-factor dLdb/Chip are critical for dorso-ventral compartmentalization in the *Drosophila* wing. *Embo J* 1998; 17: 6846–53.
- Fillmore HL, VanMeter TE, Broadbudd WC. Membrane-type matrix metalloproteinases (MT-MMPs): expression and function during glioma invasion. *J Neurooncol* 2001; 53: 187–202.
- Fink L, Seeger W, Ermert L, Hanze J, Stahl U, Grimminger F, et al. Real-time quantitative RT-PCR after laser-assisted cell picking. *Nat Med* 1998; 4: 1329–33.
- Golden JA. Cell migration and cerebral cortical development. *Neuropathol Appl Neurobiol* 2001; 27: 22–8.
- Gorter JA, van Vliet EA, Aronica E, Breit T, Rauwerda H, Lopes da Silva FH, et al. Potential new antiepileptogenic targets indicated by microarray analysis in a rat model for temporal lobe epilepsy. *J Neurosci* 2006; 26: 11083–110.
- Harduin-Leapers A, Stokes DC, Steelant WF, Samyn-Petit B, Krzewinski-Recchi MA, Vallejo-Ruiz V, et al. Cloning, expression and gene organization of a human Neu5Ac alpha 2-3Gal beta 1-3GalNAc alpha 2,6-sialyltransferase: hST6GalNAcIV. *Biochem J* 2000; 352: 37–48.
- Heinemann U. Basic mechanisms of partial epilepsies. *Curr Opin Neurol* 2004; 17: 155–9.
- Hoischen A, Ehrler M, Fassunke J, Simon M, Baudis M, Landwehr C, et al. Comprehensive characterization of genomic aberrations in gangliogliomas by comparative genomic hybridization (CGH), array-based CGH and interphase-FISH. *Brain Pathol* 2008; 18: 326–37.
- Hurd EA, Capers PL, Blauwkamp MN, Adams ME, Raphael Y, Poucher HK, et al. Loss of Chd7 function in gene-trapped reporter mice is embryonic lethal and associated with severe defects in multiple developing tissues. *Mamm Genome* 2007; 18: 94–104.
- Kanazawa M, Terada K, Kato S, Mori M. HSDJ, a human homolog of DnaJ, is farnesylated and is involved in protein import into mitochondria. *J Biochem* 1997; 121: 890–5.
- Kang HJ, Adams DH, Simen A, Simen BB, Rajkowska G, Stockmeier CA, et al. Gene expression profiling in postmortem prefrontal cortex of major depressive disorder. *J Neurosci* 2007; 27: 13329–40.
- Kim SK, Wang KC, Hong SJ, Chung CK, Lim SY, Kim YY, et al. Gene expression profile analyses of cortical dysplasia by cDNA arrays. *Epilepsy Res* 2003; 56: 175–83.
- Kiss-Toth E, Bagstaff SM, Sung HY, Jozsa V, Dempsey C, Caunt JC, et al. Human tribbles, a protein family controlling mitogen-activated protein kinase cascades. *J Biol Chem* 2004; 279: 42703–8.
- Knafo S, Grossman Y, Barkai E, Benshalom G. Olfactory learning is associated with increased spine density along apical dendrites of pyramidal neurons in the rat piriform cortex. *Eur J Neurosci* 2001; 13: 633–8.
- Kral T, Clusmann H, Blümcke I, Fimmers R, Ostertun B, Kurthen M, et al. Outcome of epilepsy surgery in focal cortical dysplasia. *J Neurol Neurosurg Psychiatry* 2003; 74: 183–8.
- Kral T, Clusmann H, Urbach J, Schramm J, Elger CE, Kurthen M, et al. Preoperative evaluation for epilepsy surgery (Bonn Algorithm). *Zentralbl Neurochir* 2002; 63: 106–10.
- Kuo TY, Hsueh YP. Expression of zinc finger transcription factor Bcl11A/Evi9/CTIP1 in rat brain. *J Neurosci Res* 2007; 85: 1628–36.
- Landau BJ, Kwaan HC, Verrusio EN, Brem SS. Elevated levels of urokinase-type plasminogen activator and plasminogen activator inhibitor type-1 in malignant human brain tumours. *Cancer Res* 1994; 54: 1105–8.
- Lukasiuk K, Kontula L, Pitkanen A. cDNA profiling of epileptogenesis in the rat brain. *Eur J Neurosci* 2003; 17: 271–9.
- Lundgren SE, Callahan CA, Thor S, Thomas JB. Control of neuronal pathway selection by the *Drosophila* LIM homeodomain gene apterous. *Development* 1995; 121: 1769–73.
- Luyken C, Blümcke I, Fimmers R, Urbach H, Elger CE, Wiestler OD, et al. The spectrum of long-term epilepsy-associated tumours: long-term

- seizure and tumour outcome and neurosurgical aspects. *Epilepsia* 2003; 44: 822–30.
- McNamara RK, Wees EA, Lenox RH. Differential subcellular redistribution of protein kinase C isozymes in the rat hippocampus induced by kainic acid. *J Neurochem* 1999; 72: 1735–43.
- Milatovic D, Zaja-Milatovic S, Montine KS, Shie FS, Montine TJ. Neuronal oxidative damage and dendritic degeneration following activation of CD14-dependent innate immune response in vivo. *J Neuroinflammation* 2004; 1: 20.
- Miller DJ, Wang Y, Kesidis G. Emergent unsupervised clustering paradigms with potential application to bioinformatics. *Front Biosci* 2008; 13: 677–90.
- Nelson BR, Claes K, Todd V, Chaverra M, Lefcort F. NELL2 promotes motor and sensory neuron differentiation and stimulates mitogenesis in DRG in vivo. *Dev Biol* 2004; 270: 322–35.
- Nicholls CD, Shields MA, Lee PW, Robbins SM, Beattie TL. UV-dependent alternative splicing uncouples p53 activity and PIG3 gene function through rapid proteolytic degradation. *J Biol Chem* 2004; 279: 24171–8.
- Niino YS, Ohno S, Suzuki K. Positive and negative regulation of the transcription of the human protein kinase C beta gene. *J Biol Chem* 1992; 267: 6158–63.
- Oh S, Iwahori A, Kato S. Human cDNA encoding DnaJ protein homologue. *Biochim Biophys Acta* 1993; 1174: 114–6.
- Ostendorff HP, Tursun B, Cornils K, Schluter A, Drung A, Gungor C, et al. Dynamic expression of LIM cofactors in the developing mouse neural tube. *Dev Dyn* 2006; 235: 786–91.
- Pace A, Bove L, Innocenti P, Pietrangeli A, Carapella CM, Oppido P, et al. Epilepsy and gliomas: incidence and treatment in 119 patients. *J Exp Clin Cancer Res* 1998; 17: 479–82.
- Parruti G, Peracchia F, Sallese M, Ambrosini G, Masini M, Rotilio D, et al. Molecular analysis of human beta-arrestin-1: cloning, tissue distribution, and regulation of expression. Identification of two isoforms generated by alternative splicing. *J Biol Chem* 1993; 268: 9753–61.
- Pfaff SL, Mendelsohn M, Stewart CL, Edlund T, Jessell TM. Requirement for LIM homeobox gene *Isl1* in motor neuron generation reveals a motor neuron-dependent step in interneuron differentiation. *Cell* 1996; 84: 309–20.
- Prayson RA. Bcl-2 and Bcl-X expression in gangliogliomas. *Hum Pathol* 1999; 30: 701–5.
- Raychaudhuri S, Sutphin PD, Chang JT, Altman RB. Basic microarray analysis: grouping and feature reduction. *Trends Biotechnol* 2001; 19: 189–93.
- Rocke DM, Durbin B. A model for measurement error for gene expression arrays. *J Comput Biol* 2001; 8: 557–69.
- Rorive S, Maris C, Debeir O, Sandras F, Vidaud M, Bieche I, et al. Exploring the distinctive biological characteristics of pilocytic and low-grade diffuse astrocytomas using microarray gene expression profiles. *J Neuropathol Exp Neurol* 2006; 65: 794–807.
- Samadani U, Judkins AR, Akpalu A, Aronica E, Crino PB. Differential cellular gene expression in ganglioglioma. *Epilepsia* 2007; 48: 646–53.
- Schick V, Majores M, Engels G, Spitoni S, Koch A, Elger CE, et al. Activation of Akt independent of PTEN and CTMP tumour-suppressor gene mutations in epilepsy-associated Taylor-type focal cortical dysplasias. *Acta Neuropathol* 2006; 112: 715–25.
- Schick V, Majores M, Fassunke J, Engels G, Simon M, Elger CE, et al. Mutational and expression analysis of CDK1, cyclinA2 and cyclinB1 in epilepsy-associated glioneuronal lesions. *Neuropathol Appl Neurobiol* 2007a; 33: 152–62.
- Schick V, Majores M, Koch A, Elger CE, Schramm J, Urbach H, et al. Alterations of phosphatidylinositol 3-kinase pathway components in epilepsy-associated glioneuronal lesions. *Epilepsia* 2007b; 48 (Suppl 5): 65–73.
- Schwartzkroin PA, Walsh CA. Cortical malformations and epilepsy. *Ment Retard Dev Disabil Res Rev* 2000; 6: 268–80.
- Sharma MK, Mansur DB, Reifenberger G, Perry A, Leonard JR, Aldape KD, et al. Distinct genetic signatures among pilocytic astrocytomas relate to their brain region origin. *Cancer Res* 2007; 67: 890–900.
- Spielman RS, Bastone LA, Burdick JT, Morley M, Ewens WJ, Cheung VG. Common genetic variants account for differences in gene expression among ethnic groups. *Nat Genet* 2007; 39: 226–31.
- Stan AD, Ghose S, Gao XM, Roberts RC, Lewis-Amezcuea K, Hatanpaa KJ, et al. Human postmortem tissue: what quality markers matter? *Brain Res* 2006; 1123: 1–11.
- Takeya R, Takeshige K, Sumimoto H. Interaction of the PDZ domain of human PICK1 with class I ADP-ribosylation factors. *Biochem Biophys Res Commun* 2000; 267: 149–55.
- Tang Y, Lu A, Aronow BJ, Wagner KR, Sharp FR. Genomic responses of the brain to ischemic stroke, intracerebral haemorrhage, kainate seizures, hypoglycemia, and hypoxia. *Eur J Neurosci* 2002; 15: 1937–52.
- Tapia-Arancibia L, Rage F, Givalois L, Arancibia S. Physiology of BDNF: focus on hypothalamic function. *Front Neuroendocrinol* 2004; 25: 77–107.
- Thom M, Martinian L, Sen A, Cross JH, Harding BN, Sisodiya SM. Cortical neuronal densities and lamination in focal cortical dysplasia. *Acta Neuropathol* 2005; 110: 383–92.
- Tsai SC, Haun RS, Tsuchiya M, Moss J, Vaughan M. Isolation and characterization of the human gene for ADP-ribosylation factor 3, a 20-kDa guanine nucleotide-binding protein activator of cholera toxin. *J Biol Chem* 1991; 266: 23053–59.
- Watanabe TK, Katagiri T, Suzuki M, Shimizu F, Fujiwara T, Kanemoto N, et al. Cloning and characterization of two novel human cDNAs (*NELL1* and *NELL2*) encoding proteins with six EGF-like repeats. *Genomics* 1996; 38: 273–6.
- Way JC, Chalfie M. *mec-3*, a homeobox-containing gene that specifies differentiation of the touch receptor neurons in *C. elegans*. *Cell* 1988; 54: 5–16.
- Williams DW, Truman JW. Mechanisms of dendritic elaboration of sensory neurons in *Drosophila*: insights from in vivo time lapse. *J Neurosci* 2004; 24: 1541–50.
- Wolf HK, Birkholz T, Wellmer J, Blümcke I, Pietsch T, Wiestler OD. Neurochemical profile of glioneuronal lesions from patients with pharmacoresistant focal epilepsies. *J Neuropathol Exp Neurol* 1995a; 54: 689–97.
- Wolf HK, Roos D, Blümcke I, Pietsch T, Wiestler OD. Perilesional neurochemical changes in focal epilepsies. *Acta Neuropathol* 1996; 91: 376–84.
- Wolf HK, Wellmer J, Muller MB, Wiestler OD, Hufnagel A, Pietsch T. Glioneuronal malformative lesions and dysembryoplastic neuroepithelial tumours in patients with chronic pharmacoresistant epilepsies. *J Neuropathol Exp Neurol* 1995b; 54: 245–54.
- Wong M. Mechanisms of epileptogenesis in tuberous sclerosis complex and related malformations of cortical development with abnormal glioneuronal proliferation. *Epilepsia* 2008; 49: 8–21.
- Wu GY, Zou DJ, Rajan I, Cline H. Dendritic dynamics in vivo change during neuronal maturation. *J Neurosci* 1999; 19: 4472–83.
- Yang YH, Dudoit S, Luu P, Lin DM, Peng V, Ngai J, et al. Normalization for cDNA microarray data: a robust composite method addressing single and multiple slide systematic variation. *Nucleic Acids Res* 2002; 30: e15.
- Yu RK, Holley JA, Macala LJ, Spencer DD. Ganglioside changes associated with temporal lobe epilepsy in the human hippocampus. *Yale J Biol Med* 1987; 60: 107–17.